PROCEEDINGS OF THE
AMERICAN MATHEMATICAL SOCIETY
Volume 142, Number 3, March 2014, Pages 737–752
S 0002-9939(2013)11807-1
Article electronically published on November 18, 2013

# A REDUCED SET OF MOVES ON ONE-VERTEX RIBBON GRAPHS COMING FROM LINKS

SUSAN ABERNATHY, CODY ARMOND, MOSHE COHEN, OLIVER T. DASBACH, HANNAH MANUEL, CHRIS PENN, HEATHER M. RUSSELL, AND NEAL W. STOLTZFUS

(Communicated by Daniel Ruberman)

Abstract. Every link in $\mathbb{R}^3$ can be represented by a one-vertex ribbon graph. We prove a Markov type theorem on this subset of link diagrams.

## 1. Introduction

A classical tool in knot theory is the Alexander polynomial. It is naturally related to Seifert surfaces (e.g. [Lic97]). For a link in braid form, the structure of the Seifert surface is particularly simple. The surface can be viewed as a series of twisted bands between a vertically stacked collection of pancake disks. Vogel gives an algorithmic proof of the classical Alexander theorem by showing that every link diagram can be transformed into a closed braid by a sequence of Reidemeister II moves [Vog90]. The Markov moves then describe the equivalence classes on braids given by the link isotopy classes of their closures [Bir74].

A strikingly similar picture is available in the Jones polynomial context. Here the natural topological objects are Turaev surfaces, which are assigned to knot diagrams [Tur87, DFK$^+$08]. Ribbon graphs encode the projection of knots on their Turaev surfaces (see the next section for definitions and discussion). Similar to the Alexander theorem, every link can be represented by a one-vertex ribbon graph. Algorithmically, this can be accomplished by using only Reidemeister II moves. In this paper we provide a Markov type theorem on one-vertex ribbon graphs.

Many celebrated knot invariants are computed via a sum over states. In other words, we assign a quantity (such as a number, polynomial, or vector space) to each state and then take an appropriate weighted sum of these quantities. Both the Alexander polynomial [Kau87a, CDR10] and the Jones polynomial [Kau87b] can be expressed in this way. Their categorified counterparts, knot-Floer homology (e.g. [MOS09]) and Khovanov homology [Kho00, BN02], also have state-sum models. We demonstrate in the final section that, for certain state sum models, these state-sum expressions simplify the subclass of one-vertex ribbon graphs.

1.1. **State diagrams, smoothings and Turaev surfaces.** Given a diagram $D$ for some link in $\mathbb{R}^3$, a state $s$ is a choice of one of the two local smoothings. These choices, called the $A$ and $B$ smoothings of a crossing, are shown in Figure 1.

Received by the editors December 21, 2011 and, in revised form, April 2, 2012.
2010 *Mathematics Subject Classification.* Primary 05C10, 57M15, 57M25.

Hence there are $2^{\#\text{ crossings in } D}$ different states $s$ for $D$ with corresponding smoothed diagrams $D_s$. The all-$A$ smoothing $D_A$ corresponds to the state where the $A$ smoothing is chosen for all crossings of $D$.

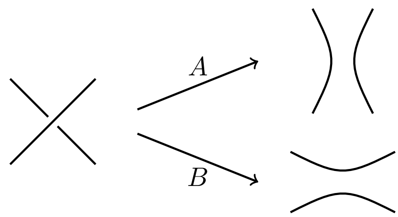


FIGURE 1. $A$ and $B$ smoothings for a link diagram

To each state $s$ with smoothed diagram $D_s$ one can naturally assign a ribbon graph $\Gamma_s$ where the vertices correspond to the circles in $D_s$ and the edges correspond to the smoothed crossings. Moreover, to each state we can associate a surface (properly embedded) in a product neighborhood of the plane in such a way that the boundary at the top and bottom correspond to the nesting of circles obtained by smoothing the state and its dual state.

Construct this surface by placing a saddle at each crossing with the zero-level corresponding to a vertex neighborhood (4-valent star) so that the corresponding smoothing for the state $s$ is obtained by the cross-section in the positive direction; see Figure 2. Connect the disjoint saddles along the edges to give a proper embedding. Finally, cap off the boundary circles with disks to obtain a closed surface. This defines the Turaev surface, denoted $\Sigma(s)$, of a state $s$. (If the state is omitted, the all-$A$ state $D_A$ is implied.) Note that the Turaev surface has a natural embedding in $S^3$ with the given link embedded in a product neighborhood of the surface.

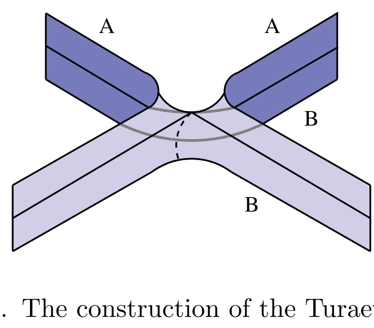


FIGURE 2. The construction of the Turaev surface

This construction has several properties which are proven in [DFK$^+$08]. For a state $s$ denote by $\bar{s}$ the state obtained by changing all $A$ smoothings to $B$ smoothings and vice versa. This is called the dual state.

**Proposition 1.1.** (1) *The Turaev surface $\Sigma(s)$ is an unknotted surface; that is, $S^3 \backslash \Sigma(s)$ is a disjoint union of two handlebodies.*
(2) *The ribbon graphs $\Gamma(s)$ and $\Gamma(\bar{s})$ can both be embedded in $\Sigma(s)$. Furthermore, $\Gamma(s)$ and $\Gamma(\bar{s})$ are dual on $\Sigma(s)$: the vertices of one correspond to the faces of the other, and the edges of one correspond to the edges of the other.*
(3) *The genera of $\Sigma(s)$, $\Gamma(s)$, and $\Gamma(\bar{s})$ are all equal.*
(4) *The projection of the link into the Turaev surface is alternating for the all-$A$ state.*

In general the all-$A$ smoothing $D_A$ will consist of several circles. The following lemma proves that every link has some diagram for which $D_A$ is a single circle and thus can be represented by a one-vertex ribbon graph [CKS11].

**Lemma 1.2** (see also [DFK+10])**.** *Every link has a diagram for which the all-$A$ smoothing consists of a single circle.*

*Proof.* If $D_A$ is a single circle no modification is necessary. If $D_A$ consists of more than one circle, then there are two distinct circles in $D_A$ that are adjacent in the sense that they can be connected by an embedded arc in $\mathbb{R}^2 - D$. (Here $\mathbb{R}^2 - D$ is the complement of the 4-valent graph underlying $D$ in the plane.) Perform a Reidemeister II move along that arc as shown in Figure 3 to obtain a new diagram $D'$.

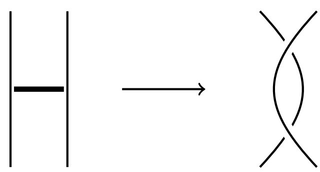


FIGURE 3. Merging circles along an arc

The all-$A$ smoothing of this new diagram, denoted $D'_A$, will have one less circle than $D_A$. In particular $D'_A$ is the result of merging the two adjacent circles from $D_A$ along the embedded arc. After finitely many iterations, this process of merging along embedded arcs will produce a diagram for which the all-$A$ smoothing is a single circle. □

The set of embedded arcs along which circles are merged is very important in the proof of the main result in this paper. For this reason, we give it the special notation $\mathcal{C}_D$ and call it a *connecting set for $D$*. Section 3 proves a technical lemma about connecting sets.

Let $\mathcal{D}$ be the set containing all diagrams for all links in $\mathbb{R}^3$; let $\widetilde{\mathcal{D}}$ be the set $\mathcal{D}$ modulo the equivalence relation induced by the three Reidemeister moves and orientation preserving isotopies in the plane. Then each $[D] \in \widetilde{\mathcal{D}}$ represents a unique link $L$ in $\mathbb{R}^3$.

Now let $\mathcal{D}_1$ be the subset of $\mathcal{D}$ consisting of diagrams for which the all-$A$ smoothing consists of a single circle. It follows from Lemma 1.2 that for each $L = [D] \in \widetilde{\mathcal{D}}$ there exists some $D' \in \mathcal{D}_1$ with $L = [D] = [D']$. In Section 2 we present a set of

Reidemeister type moves on the elements of $\mathcal{D}_1$ called $M$-moves. These $M$-moves preserve the property that the all-$A$ smoothing has a single circle.

Let $\widetilde{\mathcal{D}_1}$ be the set $\mathcal{D}_1$ under the equivalence relation induced by these new $M$-moves and orientation preserving isotopies of the plane. Consider the following two canonical mappings:

$$\phi : \mathcal{D} \to \widetilde{\mathcal{D}} \text{ and } \phi_1 : \mathcal{D}_1 \to \widetilde{\mathcal{D}_1}.$$

The first one comes from the standard Reidemeister moves, and the second one comes from the $M$-moves. In Section 4 we prove the following theorem about the relationship between $\widetilde{\mathcal{D}}$ and $\widetilde{\mathcal{D}_1}$ and their associated canonical mappings.

**Main Theorem 1.3.** *Let $D, D' \in \mathcal{D}_1$. Then $\phi(D) = \phi(D')$ if and only if $\phi_1(D) = \phi_1(D')$.*

This paper was partially inspired by Manturov's work in which the elements of $\mathcal{D}_1$ are further equipped with marked points or base points and studied as bibracket structures [Man02]. Manturov proves a theorem similar to our Main Theorem in the language of bi-bracket structures [Man02]. The moves presented here are different from those found in [Man02]. Furthermore, the fact that $M$-moves operate directly on link diagrams in the set $\mathcal{D}_1$ eliminates the need for base points.

## 2. Moves on single circle diagrams

Lemma 1.2 shows that every link in $\mathbb{R}^3$ has a diagram in the set $\mathcal{D}_1$. This section introduces a set of moves on the elements of $\mathcal{D}_1$ called $M$-moves. These moves are well-defined, meaning each move takes a diagram in $\mathcal{D}_1$ to another diagram in $\mathcal{D}_1$.

For the sake of comparison and because they will be pertinent later, the classical Reidemeister moves are listed in Figure 4. Each Reidemeister move is subdivided into two types: $a$ and $b$ based on how the number of circles in the all-$A$ smoothing changes under the move. The reader should refer back to Figure 1, which establishes the convention for the $A$ and $B$ smoothings. Observe that $R_{I_a}$ and $R_{III_a}$ preserve the number of circles in the all-$A$ smoothing, $R_{I_b}$ and $R_{II_b}$ increase the number of circles, $R_{II_a}$ decreases the number of circles, and $R_{III_b}$ can either increase or decrease the number of circles depending on connectivity.

Call the region where the Reidemeister move is being performed the distinguished region. Call the collection of points where the boundary of the distinguished region intersects the diagram distinguished points. Performing the all-$A$ smoothing outside of the distinguished region results in a collection of properly embedded arcs and circles, with the arcs connecting the distinguished points. Where it is important (such as both $R_{II}$ moves), these connections are indicated by labeling the boundary points with lowercase letters. In the case of Reidemeister I and II, notation is also introduced which distinguishes between moves and their inverses. For the remainder of the paper, Reidemeister moves are called $R$-moves.

The six moves shown in Figure 5 are called $M$-moves. As with the $R$-moves, they are local relations in the sense that $M$-moves are applied within a distinguished region, leaving the remainder of the diagram unchanged. The first move, called $M_0$, is the only $M$-move with a connectivity requirement like those found in the $R_{II_a}$ and $R_{II_b}$ in Figure 4. Connectivity requirements in $M_0$ are indicated with lowercase letters.

**Theorem 2.1.** *The $M$-moves given in Figure 5 are well-defined on the set $\mathcal{D}_1$.*

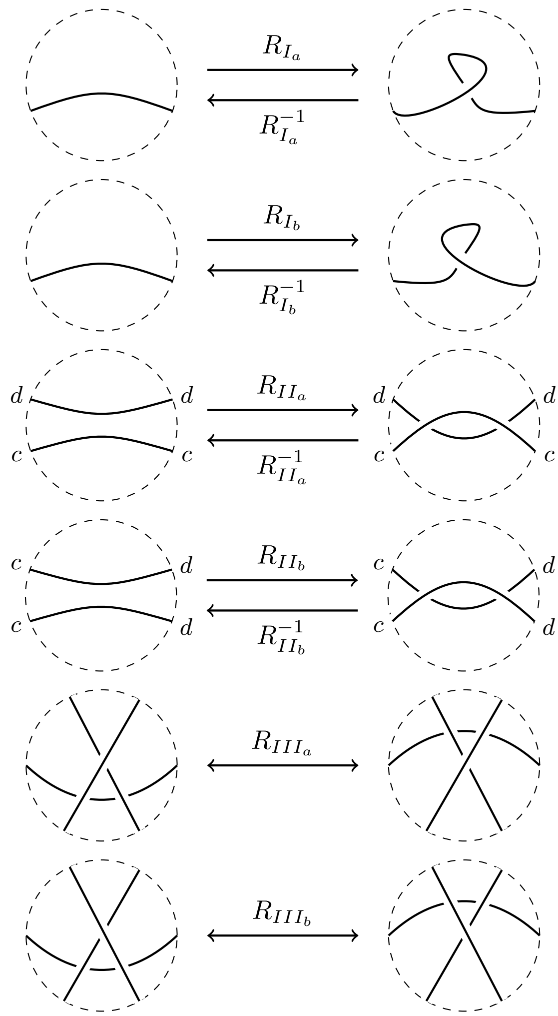


Figure 4. The $R$-moves

*Proof.* To prove this, one considers the all-$A$ smoothings within the distinguished region before and after performing each $M$-move. Each smoothing is a disjoint union of embedded arcs connecting the distinguished points pairwise.

For all but the $M_0$-move well-definedness follows from the fact that, up to isotopy, the all-$A$ smoothings in the distinguished region do not change. In the case of the $M_0$-move, the all-$A$ smoothing in the distinguished region changes, but the external connectivity requirements guarantee that the new all-$A$ smoothing will still have one circle. $\square$

## 3. Manipulating the connecting set

The proof of Lemma 1.2 makes use of the connecting set $\mathcal{C}_D$ of a diagram $D$. This section includes a technical result about the flexibility of $\mathcal{C}_D$ that is needed for the proof of the Main Theorem. Let us begin by giving a formal definition of the connecting set.

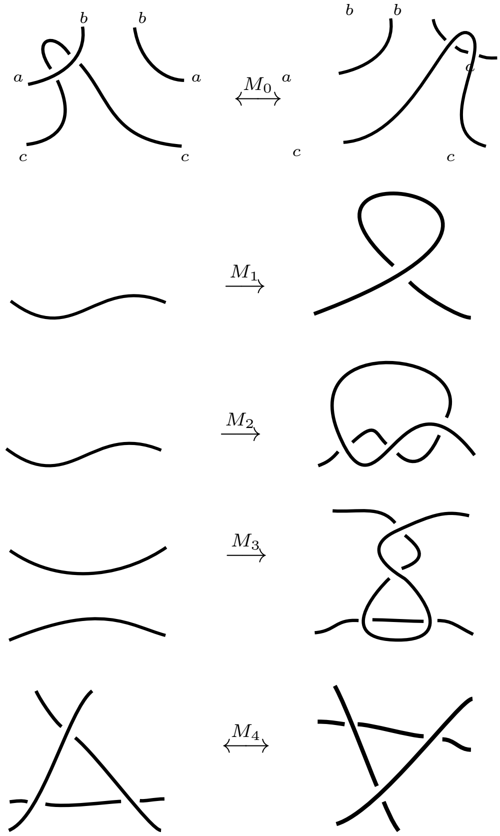


FIGURE 5. The $M$-moves

**Definition 3.1.** Let $D$ be an arbitrary link diagram. A *connecting set* $\mathcal{C}_D$ for $D$ is a minimal set of arcs embedded in $\mathbb{R}^2 - D$ with endpoints on $D$ along which performing $R_{II}$ moves yields an element of $\mathcal{D}_1$. When the diagram is clear from context, write $\mathcal{C}$ for the connecting set; in particular, denote by $D_{\mathcal{C}}$ the modification of $D$ prescribed by $\mathcal{C}$. This diagram is always in $\mathcal{D}_1$.

Part of the definition of the connecting set is that the arcs it contains must lie in $\mathbb{R}^2 - D$, so these arcs cannot intersect the locations of crossings from $D$. As elements of the connecting set are manipulated, it is imperative to pay attention to these crossings. The following notation aids in this task.

**Definition 3.2.** A *crossing arc* is an embedded arc in $\mathbb{R}^2 - D_A$ that marks the location of a crossing from $D$. A set of crossing arcs, one for each crossing of $D$, will be called a *crossing set* and will be denoted by $\mathcal{X}_D$.

Throughout the remaining figures in the paper, elements of the connecting set $\mathcal{C}_D$ will be given by thick solid lines, and elements of the crossing set $\mathcal{X}_D$ will be given by dotted lines. In Figure 6 a portion of a diagram $D$ is shown alongside the corresponding all-$A$ smoothing decorated with a crossing arc. Unlike the connecting

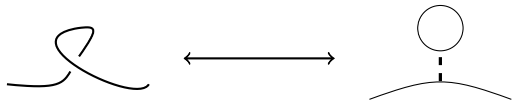

FIGURE 6. Crossing arc

set, the crossing set for $D$ is unique. Given $D_A$ and the crossing set $\mathcal{X}_D$, we can reconstruct the diagram $D$ up to isotopy. Moreover, note that $\mathbb{R}^2 - D$ is homeomorphic to $R^2 - (D_A \cup \mathcal{X}_D)$.

**Lemma 3.3.** *Let $D \in \mathcal{D}$, and let $\mathcal{C}$ be an arbitrary connecting set for $D$. If $x, y \in D$ are points on distinct circles in $D_A$ connected by an embedded arc $s \in \mathbb{R}^2 - D$ that does not intersect any of the elements in $\mathcal{C}$, then there is another connecting set $\mathcal{C}'$ for $D$ such that*

(1) *$s \in \mathcal{C}'$ and*
(2) *the diagrams $D_{\mathcal{C}}$ and $D_{\mathcal{C}'}$ are equivalent via $M_0$-moves.*

*Proof.* Begin by noting that the elements of $\mathcal{C}$ are actually contained in $\mathbb{R}^2 - D_A$. In other words, elements of the connecting set can be viewed as arcs connecting circles in the all-$A$ smoothing.

Now consider the union $U = D_A \cup \mathcal{C}$ embedded in $\mathbb{R}^2$ as well as its complement $V = \mathbb{R}^2 - U$. The set $V$ will consist of a collection of components in the plane, each of which has boundary comprised of some combination of arcs which will alternate between elements of $\mathcal{C}$ and portions of circles in $D_A$. Each bounded component of $V$ is contractible since $U$ is connected.

Since $s$ does not intersect any elements of $\mathcal{C}$ it lies inside a single component $P$ of $V$. Furthermore, $P - s$ will contain two components. At least one of these two components is bounded and contractible. Call it $P'$.

The boundary of $P'$ will consist of arcs in $\mathcal{C}$, portions of circles in $D_A$, and the arc $s$. Think of this boundary as being a polygon with an even number of sides, every other side being a portion of some circle in $D_A$. As we travel along the boundary of $P'$ some arcs in $\mathcal{C}_D$ will be traversed twice. Such arcs are called *internal arcs*. The others (ones that separate $P'$ from other components of $V - s$) will be called *external arcs*. Give $P'$ an orientation. This induces an orientation on the boundary of $P'$ and thus on the external arcs. In the figures illustrating various cases of the proof, external arcs are drawn with their orientations, while internal arcs and arcs outside $P'$ are unoriented.

Let $m_e$ be the number times a connecting arc is traversed as one travels the boundary of $P'$ so that each internal edge is counted twice, while external edges are counted once. Let $m_c$ be the number of crossing arcs inside $P'$, and let $m = m_e + m_c$.

The proof proceeds by giving an algorithm which modifies the link diagram and the polygon $P'$, reducing $m$ at each step. This algorithm changes elements of the connecting set, thus producing a sequence of connecting sets $\mathcal{C} = \mathcal{C}_0, \mathcal{C}_1, \ldots, \mathcal{C}_n$ and an associated sequence of diagrams $D_{\mathcal{C}} = D_{\mathcal{C}_0}, \ldots, D_{\mathcal{C}_n}$. On the level of the diagrams each of the operations we define comes from the application of an $M_0$ move.

Eventually these operations reduce $P'$ to a square for which $m_e = 2$ and $m_c = 0$. In other words, after the final step, $P'$ contains no crossing arcs and is bounded by two segments of circles from $D_A$, one arc in $\mathcal{C}_n$ and the special arc $s$. This means that the arc in $\mathcal{C}_n$ and the arc $s$ are isotopic. Therefore by performing this isotopy we may take $\mathcal{C}_n = \mathcal{C}'$, and the lemma is proven.

Step 1 proceeds as follows. Begin by choosing the first external arc $s'$ from $\mathcal{C}_{i-1}$ that appears in the oriented boundary of $P'$ after the arc $s$. Note that while $s'$ is the first external arc, it is possible that there are some internal arcs in the oriented boundary of $P'$ between $s$ and $s'$. If such arcs exist, they are connected to circles with boundary also appearing in the oriented boundary of $P'$ between $s$ and $s'$. See Figure 7 for an example of such a situation.

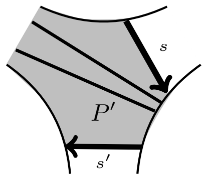


FIGURE 7. Internal arcs between $s$ and $s'$

Next, examine the circle on which the head of $s'$ is incident. Traveling from the head of $s'$ along the circle inside of $P'$ one of three things will be encountered:

(1) a crossing arc from $\mathcal{X}_D$ in $P'$,
(2) a connecting arc from $\mathcal{C}_{i-1}$ that is part of the boundary of $P'$,
(3) or the arc $s$.

Before examining these cases, a fourth omitted possibility should be mentioned. We could encounter a crossing arc or connecting arc with an endpoint on the circle lying in a region adjacent to $P'$. In this case, an $M_0$ move can be used to "jump over" the endpoints of these arcs. Furthermore there are only finitely many of these points, so it will not prevent our algorithm from terminating. Figure 8 shows a picture of this situation.

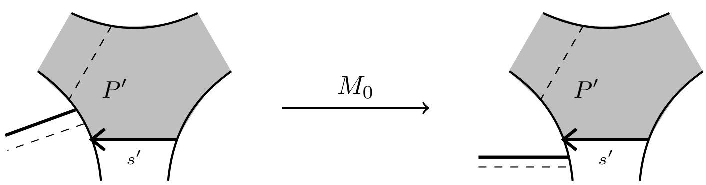


FIGURE 8. Jumping over crossing and connecting arcs not in $P'$

*Case* 1. The arc following $s'$ is a crossing arc from $\mathcal{X}_D$ in $P'$.

In this situation there are four possibilities:

a. The crossing arc is parallel to $s'$ with no crossing arcs, connecting arcs, or elements of $D_A$ between them.
b. The crossing arc and $s'$ are parallel with some crossing arcs, connecting arcs, or elements of $D_A$ between them.
c. The crossing arc is not parallel to $s'$ and joins two circles that lie in different connected components of $U - \{s'\}$.
d. The crossing arc is not parallel to $s'$ and joins two circles that lie in the same connected component of $U - \{s'\}$.

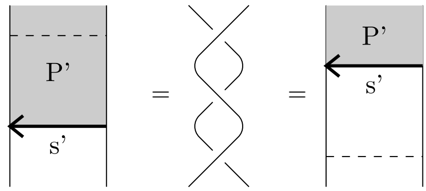


FIGURE 9. Case 1a: A connecting arc and a crossing are switched

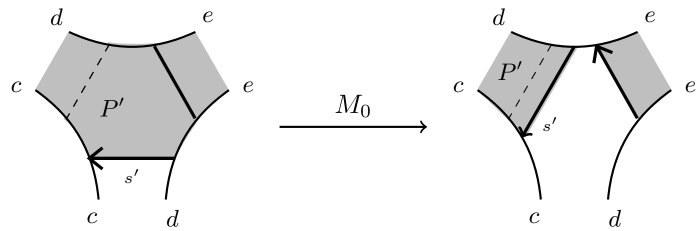


FIGURE 10. Case 1c: Removing $s'$ disconnects the leftmost circle

In Case 1a the positions of the arc and the crossing can be exchanged without changing the diagram $D_{\mathcal{C}_{i-1}}$, as shown in Figure 9. This reduces $m_c$.

In Case 1b, any arcs or elements of $D_A$ lying between the crossing arc and $s'$ must be anchored beside the tail of $s'$ inside $P'$. Using an $M_0$ move, reposition the tail of $s'$ so that the collection of crossing arcs, connecting arcs, and circles from $D_A$ are no longer in $P'$. The crossing arc and $s'$ will then be parallel with nothing in between them. This reduces at least one of $m_e$ and $m_c$.

In Case 1c, the crossing arc joins two circles in different connected components of $U - \{s'\} = (D_a \cup \mathcal{C}_{i-1}) - \{s'\}$. Since the connecting set is minimal, removing $s'$ breaks $U$ into two connected components. The crossing arc in this case has endpoints in both of these components. This must mean that the crossing arc is connected to a circle that appears in the boundary of $P'$ between $s$ and $s'$, and the only way that this can happen is if there are some internal arcs in the boundary of $P'$ between $s$ and $s'$. Perform an $M_0$ move on the arc $s'$ leaving the head fixed while moving the tail so that $s'$ and the crossing arc are now parallel as shown in Figure 10. This will reduce $m_e$ since at least one internal arc between $s$ and $s'$ will become an external arc.

In Case 1d, the crossing arc joins two circles in the same connected component of $U-\{s'\}$. Unlike the previous case, the crossing arc has both endpoints on the same component of $U - \{s'\}$. This means that the crossing arc connects two circles that both occur in the boundary of $P'$ after $s'$. An $M_0$ move can still be performed, but this time leave the tail of $s'$ fixed and move the head to a position adjacent to the other end of the crossing arc as shown in Figure 11. This reduces $m_c$ by removing the crossing arc from $P'$. It also may reduce $m_e$, depending on the structure of $P'$.

*Case* 2. The arc after $s'$ is another connecting arc from $\mathcal{C}_{i-1}$.

In this situation, there are two possibilities:

a. the arc is internal or
b. the arc is external.

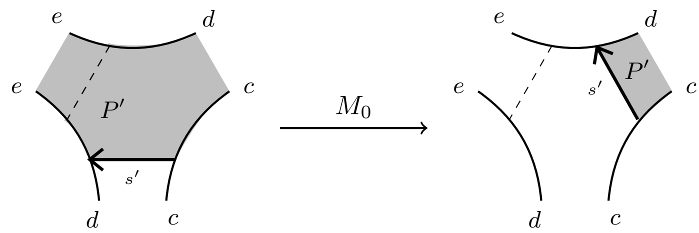


FIGURE 11. Case 1d: Removing $s'$ disconnects the rightmost circle

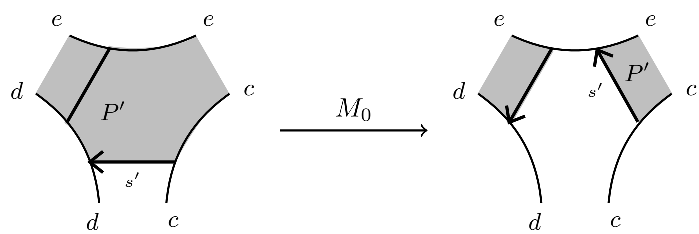


FIGURE 12. Case 2a: $s'$ is followed by an internal arc

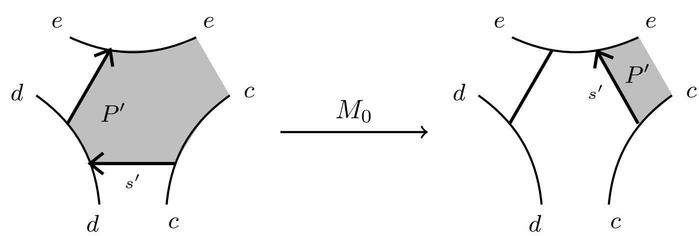


FIGURE 13. Case 2b: $s'$ is followed by an external arc

In both Cases 2a and 2b, the two circles joined by the arc we encounter are in the same connected component of $U - \{s'\}$. Perform an $M_0$ move, leaving the tail of $s'$ fixed and moving the head as shown in Figure 12 for Case 2a and in Figure 13 for Case 2b. In Case 2a, this will change at least one internal edge to an external edge, so $m_e$ will go down. In Case 2b, an external edge is removed from the boundary of $P'$, so again $m_e$ goes down.

*Case* 3. The arc we encounter is $s$.

In this situation, there are two possibilities:

a. the arcs $s$ and $s'$ are parallel with nothing between them or
b. the arcs $s$ and $s'$ are parallel with some undirected arcs, crossing arcs, and circles from $D_A$ between them.

These two possibilities are analogous to Cases 1a and 1b. In Case 3a since $s$ and $s'$ are isotopic, assume that $s$ replaces $s'$ in the connecting set, and the proof is complete. In Case 3b, perform an $M_0$ move to remove the undirected arcs, crossing arcs, and circles from $P'$. This will reduce either $m_c$ or $m_e$, depending on what was between $s$ and $s'$. □

## 4. A Reidemeister type theorem on one-vertex ribbon graphs

Recall that the equivalence relations induced by $R$-moves and $M$-moves respectively yield the following two canonical mappings:

$$\phi : \mathcal{D} \to \widetilde{\mathcal{D}} \qquad \text{and} \qquad \phi_1 : \mathcal{D}_1 \to \widetilde{\mathcal{D}_1}.$$

This section proves the following theorem, which says that we can completely characterize the isotopy classes of links in $\mathbb{R}^3$ by restricting our focus to diagrams in $\mathcal{D}_1$ modulo $M$-moves.

**Main Theorem 4.1.** *Let $D, D' \in \mathcal{D}_1$. Then $\phi(D) = \phi(D')$ if and only if $\phi_1(D) = \phi_1(D')$.*

One direction of the proof follows immediately from the definition of the $M$-moves. Indeed the following statement can be verified by examining the pictures of the $M$-moves in Figure 5.

**Lemma 4.2.** *Given $D, D' \in \mathcal{D}_1$, if $\phi_1(D) = \phi_1(D')$, then $\phi(D) = \phi(D')$.*

*Proof.* If $\phi_1(D) = \phi_1(D')$, then $D$ can be transformed to $D'$ through a sequence of $M$-moves. Examining the $M$-moves in Figure 5, it is clear that each of them can be expressed as a sequence of $R$-moves. Since $D$ and $D'$ are related by a sequence of $R$-moves, it follows that $\phi(D) = \phi(D')$. □

**Theorem 4.3.** *Say $D, D' \in \mathcal{D}_1$ such that $\phi(D) = \phi(D')$. Then $\phi_1(D) = \phi_1(D')$. In other words, two diagrams in $\mathcal{D}_1$ that are related by a sequence of $R$-moves are also related by a sequence of $M$-moves.*

*Proof.* If $\phi(D) = \phi(D')$, then there exists a sequence of diagrams

$$D = D_0 \xrightarrow{R_0} D_1 \xrightarrow{R_1} \cdots \xrightarrow{R_{m-2}} D_{m-1} \xrightarrow{R_{m-1}} D_m = D'.$$

In this context each pair of diagrams $D_i$ and $D_{i+1}$ differs by a single $R$-move, denoted $R_i$.

The proof proceeds by reinterpreting each move $R_i$ as a sequence of $M$-moves and building a connecting set $\mathcal{C}_i$ associated to each diagram $D_i$. Note that since $D, D' \in \mathcal{D}_1$ it follows that $\mathcal{C}_0 = \mathcal{C}_m = \emptyset$. Therefore, this proof describes a sequence

$$(D_0)_\emptyset \to (D_1)_{\mathcal{C}_1} \to \cdots \to (D_i)_{\mathcal{C}_i} \to \cdots \to (D_{m-1})_{\mathcal{C}_{m-1}} \to (D_m)_\emptyset$$

where each arrow is either the identity or a sequence of $M$-moves.

We consider the $R$-moves listed in Figure 4 and show how each of these can be reinterpreted in terms of a collection of $M$-moves. Each case begins with diagrams $D_i$ and $D_{i+1}$, a connecting set $\mathcal{C}_i$ for $D_i$, and an $R$-move $R_i$ that takes $D_i$ to $D_{i+1}$. Using a combination of isotopy and repeated applications of Lemma 3.3, a connecting set $\mathcal{C}_{i+1}$ is constructed to accompany the diagram $D_{i+1}$. Sometimes it is also necessary to have intermediate diagrams and connecting sets. There are ten cases.

**Case 1:** $R_i$ is an $R_{I_a}$-move. Note that $R_{I_a}$ is just the move $M_1$. Using isotopy, move any elements of $\mathcal{C}_i$ away from the distinguished region. Since an application of $R_{I_a}$ does not change the number of circles in the all-$A$ smoothing, $\mathcal{C}_i$ is also a connecting set for $D_{i+1}$. Set $\mathcal{C}_{i+1} = \mathcal{C}_i$ and $M_i = R_i$.

**Case 2:** $R_i$ is an $R_{I_a}^{-1}$-move. Note that $R_{I_a}^{-1}$ is just $M_1^{-1}$. There are finitely many connecting arcs incident on the loop that $R_i$ removes. By applying a sequence of $M_0$ moves, move elements of $\mathcal{C}_i$ out of the distinguished region, obtaining a new connecting set for $D_i$ called $\mathcal{C}_i'$. Set $\mathcal{C}_{i+1} = \mathcal{C}_i'$ and $M_i = R_i$.

**Case 3:** $R_i$ is an $R_{I_b}$-move. In this case the number of circles in $(D_i)_A$ is one less than $(D_{i+1})_A$, so the connecting set $\mathcal{C}_{i+1}$ should have one more arc than the connecting set $\mathcal{C}_i$. Using isotopy, move any elements of $\mathcal{C}_i$ out of the distinguished region. Now let $\mathcal{C}_{i+1} = \mathcal{C}_i \cup \{s\}$, where the arc $s$ is shown in Figure 14. Then $(D_{i+1})_{\mathcal{C}_{i+1}}$ is related to $(D_i)_{\mathcal{C}_i'}$ via the move $M_2$.

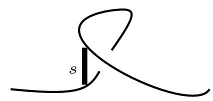


FIGURE 14. $M_2$ is $R_{Ib}$ with an extra connecting arc $s$

**Case 4:** $R_i$ is an $R_{I_b}^{-1}$-move. Begin by invoking Lemma 3.3 to get the element $s$ of the connecting set shown in Figure 14. This forms a new connecting set $\mathcal{C}_i'$. There may be other elements of the connecting set attached to the loop being removed by the move $R_i$. These can be moved off the loop using a sequence of $M_0$ moves. Call this further modified connecting set $\mathcal{C}_i''$. Then let $\mathcal{C}_{i+1} = \mathcal{C}_i'' - \{s\}$. The diagram $(D_{i+1})_{\mathcal{C}_{i+1}}$ is related to $(D_i)_{\mathcal{C}_i'}$ via the move ${M_2}^{-1}$.

**Case 5:** $R_i$ is an $R_{IIa}$-move. There may be some number of parallel connecting arcs from $\mathcal{C}_i$ that run through the "corridor" where the $R_i$ is being performed. Beginning with the leftmost arc, move each arc out of the corridor via an $M_0$-move that places one of its two endpoints on the left-hand circle involved in the distinguished region. Repeat this until all connecting arcs have been removed from the corridor. This produces a new connecting set $\mathcal{C}_i'$. Once the corridor is cleared, invoke Lemma 3.3 to get a new connecting set containing the arc $s$ shown in Figure 3. Call this further modified connecting set $\mathcal{C}_i''$. Let $\mathcal{C}_{i+1} = \mathcal{C}_i'' - \{s\}$. The diagram $(D_{i+1})_{\mathcal{C}_{i+1}}$ is the same as $(D_i)_{\mathcal{C}_i''}$.

**Case 6:** $R_i$ is an $R_{IIa}^{-1}$-move. Use $M_0$-moves to move any connecting arcs out of the distinguished region. This produces a new connecting set $\mathcal{C}_i'$. Let $\mathcal{C}_{i+1} = \mathcal{C}_i' \cup \{s\}$, where $s$ is the connecting arc shown in Figure 3. Then as in the previous case, the diagram $(D_{i+1})_{\mathcal{C}_{i+1}}$ is the same as $(D_i)_{\mathcal{C}_i'}$.

**Case 7:** $R_i$ is an $R_{IIb}$-move. As in Case 5, there may be some number of parallel connecting arcs running through the "corridor" where $R_i$ is to be performed. Using the same process, a sequence of $M_0$-moves will remove all connecting arcs from the corridor producing a new connecting set $\mathcal{C}_i'$. Now let $\mathcal{C}_{i+1} = \mathcal{C}_i' \cup \{s\}$ where $s$ is the arc shown in Figure 15. Then $(D_i)_{\mathcal{C}_i'}$ is related to $(D_{i+1})_{\mathcal{C}_{i+1}}$ via the move $M_3$.

**Case 8:** $R_i$ is an $R_{IIb}^{-1}$-move. Begin by using $M_0$-moves to clear any connecting arcs from the distinguished region. This yields a new connecting set $\mathcal{C}_i'$. Then invoke Lemma 3.3 to get a new connecting set $\mathcal{C}_i''$ containing the arc $s$ shown in Figure 15. Let $\mathcal{C}_{i+1} = \mathcal{C}_i'' - \{s\}$. Then $(D_i)_{\mathcal{C}_i'}$ is related to $(D_{i+1})_{\mathcal{C}_{i+1}}$ via the move $M_3^{-1}$.

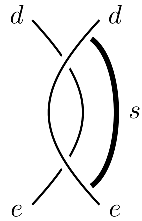


FIGURE 15. The connecting arc $s$ for $R_{IIb}$

**Case 9:** $R_i$ is an $R_{IIIa}$-move. First use isotopy and possibly some $M_0$-moves to move any connecting arcs out of the distinguished region except for a possible connecting arc in the triangular region enclosed by the three crossings involved in the move. This yields a new connecting set $\mathcal{C}'_i$.

If there is a connecting arc within that triangular region, it will be one of the two shown in Figure 16. Invoke Lemma 3.3 to get another arc $s$, which is also shown in Figure 16. Call this new connecting set $\mathcal{C}''_i$. Since both the arc in the triangular region and the arc $s$ connect the same circles in $(D_i)_A$, the connecting arc within the triangular region will not be present in $\mathcal{C}''_i$. Now let $\mathcal{C}''_i = \mathcal{C}_{i+1}$. Then $(D_i)_{\mathcal{C}''_i}$ and $(D_{i+1})_{\mathcal{C}_{i+1}}$ are related by the move $M_4$.

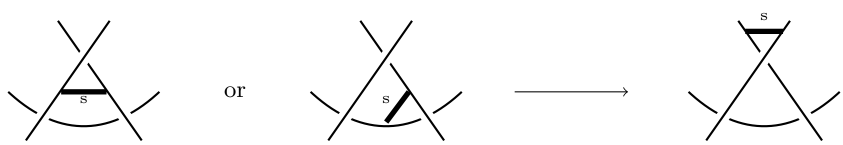


FIGURE 16. A connecting arc in the triangular region can be replaced by $s$

**Case 10:** $R_i$ is an $R_{IIIb}$-move. This move can be written as the composition of two $R_{II}$-moves and an $R_{IIIa}$-move, so this case is covered by previous arguments. $\square$

## 5. EXAMPLE

This section gives an example of the algorithm outlined in the proof of Theorem 4.3. Figure 17 shows a sequence of $R$-moves performed on the unknot. This sequence begins and ends with elements of $\mathcal{D}_1$, so the Main Theorem tells us that there exists a sequence of $M$-moves taking the first diagram to the last. This is shown in Figure 18.

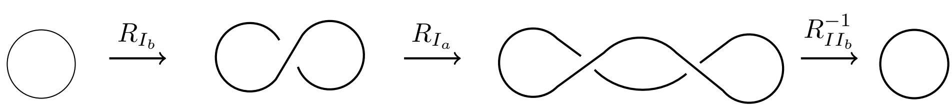


FIGURE 17. A sequence of $R$-moves taking the crossingless unknot to itself

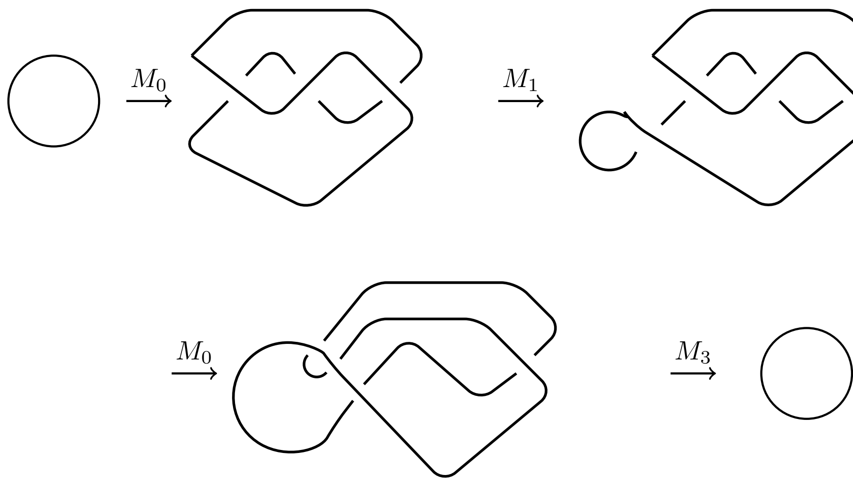


FIGURE 18. A sequence of $M$-moves taking the crossingless unknot to itself

## 6. Application

As pointed out in the introduction, one can assign to each knot diagram a ribbon graph $\Gamma$, i.e. a graph with an embedding on an orientable surface from which the knot can be recovered (up to reversing the orientation of the ambient space) [DFK+08]. For an alternating knot with an alternating diagram the graph is planar, and this characterizes alternating knots. Bollobás and Riordan [BR01] introduced a three variable extension to ribbon graphs $C(X, Y_{BR}, Z; \Gamma)$ of the Tutte polynomial $T(X, Y_T; G)$. For a ribbon graph $\Gamma$ whose underlying graph $G_\Gamma$ is obtained by forgetting the embedding of $\Gamma$, one has

$$C(X, Y_{BR}, 1; \Gamma) = T(X, Y_{BR} + 1; G_\Gamma).$$

For a knot diagram with associated ribbon graph $\Gamma$ the evaluation

$$C(-A^4, -A^{-4} - 1, (-A^2 - A^{-2})^{-2}; \Gamma)$$

yields the Kauffman bracket of the knot diagram [DFK+08], which is, up to normalizations and variable change, the Jones polynomial of the knot. In the case of one-vertex ribbon graphs $\Gamma$ the Bollobás-Riordan-Tutte polynomial simplifies significantly and becomes a two variable polynomial $C(-, Y_{BR}, Z; \Gamma)$ [BR01].

Note that in [CKS11] an expansion of the Bollobás-Riordan-Tutte polynomial over certain sub-ribbon graphs called quasi-trees is given (see also [DFK+10]). This expansion is simplified significantly for one-vertex ribbon graphs.

Furthermore, in [DL11] a Khovanov homology theory for ribbon graphs is worked out that coincides with the regular Khovanov homology if the ribbon graph comes from a knot diagram. It will be interesting to see what simplifications the restriction to the one-vertex case gives.

## Acknowledgments

This project is the outcome of a semester-long NSF-VIGRE research course in knot theory at LSU. The authors are grateful to VIGRE for providing the organizational resources that made this research possible.

The third and seventh authors were partially supported by NSF VIGRE grant DMS 0739382.

The fourth author was supported in part by NSF grants DMS-0806539 and DMS-0456275 (FRG).

The eighth author was also supported by DMS-0456275 (FRG).

Finally, the authors thank the referee for helpful suggestions.

## References

[Bir74] Joan S. Birman, *Braids, links, and mapping class groups*, Annals of Mathematics Studies, No. 82, Princeton University Press, Princeton, N.J., 1974. MR0375281 (51 #11477)

[BN02] Dror Bar-Natan, *On Khovanov's categorification of the Jones polynomial*, Algebr. Geom. Topol. **2** (2002), 337–370 (electronic), DOI 10.2140/agt.2002.2.337. MR1917056 (2003h:57014)

[BR01] Béla Bollobás and Oliver Riordan, *A polynomial invariant of graphs on orientable surfaces*, Proc. London Math. Soc. (3) **83** (2001), no. 3, 513–531, DOI 10.1112/plms/83.3.513. MR1851080 (2002f:05056)

[CDR10] Moshe Cohen, Oliver T. Dasbach, and Heather M. Russell, *A twisted dimer model for knots*, arXiv:1010.5228v2 (2010), 1–16.

[CKS11] Abhijit Champanerkar, Ilya Kofman, and Neal Stoltzfus, *Quasi-tree expansion for the Bollobás-Riordan-Tutte polynomial*, Bull. Lond. Math. Soc. **43** (2011), no. 5, 972–984, DOI 10.1112/blms/bdr034. MR2854567

[DFK+08] Oliver T. Dasbach, David Futer, Efstratia Kalfagianni, Xiao-Song Lin, and Neal W. Stoltzfus, *The Jones polynomial and graphs on surfaces*, J. Combin. Theory Ser. B **98** (2008), no. 2, 384–399, DOI 10.1016/j.jctb.2007.08.003. MR2389605 (2009d:57020)

[DFK+10] Oliver T. Dasbach, David Futer, Efstratia Kalfagianni, Xiao-Song Lin, and Neal W. Stoltzfus, *Alternating sum formulae for the determinant and other link invariants*, J. Knot Theory Ramifications **19** (2010), no. 6, 765–782, DOI 10.1142/S021821651000811X. MR2665767 (2011d:57010)

[DL11] Oliver T. Dasbach and Adam M. Lowrance, *A Turaev surface approach to Khovanov homology*, arXiv:1107.2344 (2011), 1–30.

[Kau87a] Louis H. Kauffman, *On knots*, Annals of Mathematics Studies, vol. 115, Princeton University Press, Princeton, NJ, 1987. MR907872 (89c:57005)

[Kau87b] Louis H. Kauffman, *State models and the Jones polynomial*, Topology **26** (1987), no. 3, 395–407, DOI 10.1016/0040-9383(87)90009-7. MR899057 (88f:57006)

[Kho00] Mikhail Khovanov, *A categorification of the Jones polynomial*, Duke Math. J. **101** (2000), no. 3, 359–426, DOI 10.1215/S0012-7094-00-10131-7. MR1740682 (2002j:57025)

[Lic97] W. B. Raymond Lickorish, *An introduction to knot theory*, Graduate Texts in Mathematics, vol. 175, Springer-Verlag, New York, 1997. MR1472978 (98f:57015)

[Man02] V. O. Manturov, *Knots and the bracket calculus*, Acta Appl. Math. **74** (2002), no. 3, 293–336, DOI 10.1023/A:1021154925574. MR1942533 (2003j:57012)

[MOS09] Ciprian Manolescu, Peter Ozsváth, and Sucharit Sarkar, *A combinatorial description of knot Floer homology*, Ann. of Math. (2) **169** (2009), no. 2, 633–660, DOI 10.4007/annals.2009.169.633. MR2480614 (2009k:57047)

[Tur87] V. G. Turaev, *A simple proof of the Murasugi and Kauffman theorems on alternating links*, Enseign. Math. (2) **33** (1987), no. 3-4, 203–225. MR925987 (89e:57002)

[Vog90] Pierre Vogel, *Representation of links by braids: a new algorithm*, Comment. Math. Helv. **65** (1990), no. 1, 104–113, DOI 10.1007/BF02566597. MR1036132 (90k:57013)

Department of Mathematics, Louisiana State University, Baton Rouge, Louisiana 70803

*E-mail address*: sabern1@tigers.lsu.edu

Department of Mathematics, Louisiana State University, Baton Rouge, Louisiana 70803

*Current address*: Department of Mathematics, The University of Iowa, Iowa City, Iowa 52242

*E-mail address*: cody-armond@uiowa.edu

Department of Mathematics, Bar-Ilan University, Ramat Gan 52900, Israel

*E-mail address*: cohenm10@macs.biu.ac.il

Department of Mathematics, Louisiana State University, Baton Rouge, Louisiana 70803

*E-mail address*: kasten@math.lsu.edu

Department of Mathematics, Louisiana State University, Baton Rouge, Louisiana 70803

*Current address*: Department of Mathematics, Georgia Institute of Technology, Atlanta, Georgia 30332

*E-mail address*: hmanuel3@math.gatech.edu

Department of Mathematics, Louisiana State University, Baton Rouge, Louisiana 70803

*E-mail address*: coffee@math.lsu.edu

Department of Mathematics, University of Southern California, Los Angeles, California 90089-2532

*Current address*: Department of Mathematics and Computer Science, Washington College, Chestertown, Maryland 21620

*E-mail address*: hrussell2@washcoll.edu

Department of Mathematics, Louisiana State University, Baton Rouge, Louisiana 70803

*E-mail address*: stoltz@math.lsu.edu